International Journal of Mechanical, Industrial and Aerospace Sciences
ISSN: 2517-9950
Vol:10, No:4, 2016

Nonlinear Structural Behavior of Micro- and Nano-Actuators Using the Galerkin Discretization Technique

Hassen M. Ouakad

***Abstract*—**In this paper, the influence of van der Waals, as well as electrostatic forces on the structural behavior of MEMS and NEMS actuators, has been investigated using of a Euler-Bernoulli beam continuous model. In the proposed nonlinear model, the electrostatic fringing-fields and the mid-plane stretching (geometric nonlinearity) effects have been considered. The nonlinear integro-differential equation governing the static structural behavior of the actuator has been derived. An original Galerkin-based reduced-order model has been developed to avoid problems arising from the nonlinearities in the differential equation. The obtained reduced-order model equations have been solved numerically using the Newton-Raphson method. The basic design parameters such as the pull-in parameters (voltage and deflection at pull-in), as well as the detachment length due to the van der Waals force of some investigated micro- and nano-actuators have been calculated. The obtained numerical results have been compared with some other existing methods (finite-elements method and finite-difference method) and the comparison showed good agreement among all assumed numerical techniques.

***Keywords*—**MEMS, NEMS, fringing-fields, mid-plane stretching, Galerkin method.

I. Introduction

RECENTLY, the field of micro- and nanostructures has started to lead as a significant and promising representative for exceptional technology that has resulted in major changes in many industries. These micro- and nano-scale devices have shown to be very promising in replacing bulky macro-scale actuators and sensors by reducing manufacturing costs, the bulkiness of the prototyped systems, and effectively decreasing weight and power consumption, while increasing overall performance, production volume, and functionality. These advantages have led to the field of micro- and nano-electromechanical systems (MEMS and NEMS) to generate substantial interest in the scientific community in recent years. MEMS technology has already had a significant impact on the areas of medical, automotive, aerospace, and sensors and actuators technology [1]-[6]. Some prospective applications of NEMS include random access memory, nano-tweezers, and super-sensitive sensors [7]-[10], etc.

There are some basic differences in modeling the behavior of MEMS and NEMS structures. For example, the van der Waals force interactions, which can be neglected when designing MEMS structures, are in fact prominent in some NEMS devices [11].

H. M. Ouakad is with the Mechanical Engineering Department, King Fahd University of Petroleum and Minerals, Dhahran, 31261 Kingdom of Saudi Arabia (e-mail: houakad@kfupm.edu.sa).

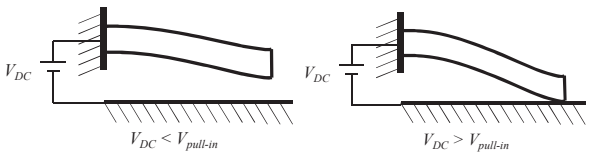

(a) (b)

Fig. 1 Parallel-plates DC electrostatic actuation and the pull-in instability

The majority of MEMS and NEMS devices showed high interest in using the electrostatic field as a prominent actuation method. Among the numerous electrostatic actuation methods for these tiny devices, the parallel-plates method is the most reputable technique because of its simplicity and high efficiency [12]. It is the most common actuation method, where, a movable micro- or nano-electrode is deflected under the effect of an electrostatic load of V_{DC} applied through a fixed electrode (the gate), Fig. 1 (a). In this simple actuation method, the electric charge generates an electric field around it. Then, the electric field creates a force on the charged particle. Since, the electric charge generates an electric field around the two electrodes; the field creates an electrostatic force on the electrodes. As the electric load increases, the movable electrode deflects and moves towards the stationary one, Fig. 1 (a). If the electrostatic voltages exceed a certain limit value, this leads to a sudden failure (inherent instability) of the structure in which the movable electrode hits the stationary electrode, Fig. 1 (b). This happens because the microbeam's restoring force can no longer resist the contrasting electrostatic force. This structural instability phenomenon is known as *pull-in* and the associated voltage is called pull-in voltage ($V_{pull\text{-}in}$) [13], [14]. The corresponding gap is called the pull-in deflection. Voltage and deflection in this state together are also called the pull-in parameters of the MEMS/NEMS actuator. This phenomenon may be considered as a desirable (mainly for switches) or an undesirable (mainly for resonators) phenomenon; so there is a need to calculate exactly the pull-in parameters. Many studies have addressed the pull-in phenomenon and presented tools to predict its occurrence, enabling MEMS and NEMS designers to depict it accurately [13]-[20]. Nevertheless, many studies [21]-[25], especially in the NEMS field, did not investigate carefully

some key parameters that may influence the exact extraction of the pull-in parameters for a nanostructure. For example, Dequesnes et al. [21] calculated numerically the pull-in voltage of carbon nanotubes based NEMS switches considering the effects of the van der Waals effects; however, omitting its influence on the pull-in gap. Another group [22], [23] studied the adhesion problem of two single-walled carbon nanotubes and the collapse of one single-walled carbon nanotube based on continuum analysis. Both studies concluded the significant influence of the van der Waals force on the structural stability of single-walled carbon nanotubes. Another group [24] studied the structural behavior of NEMS actuators assuming the Casimir effect. They determined the needed detachment length of the nano-switches to not stick to the substrate. Wang et al. [25] used Galerkin-based reduced-order modeling to discretize the governing equations for the pull-in of carbon nano-tweezers under the effect of van der Waals forces.

From the above mentioned investigations, one can note that a robust and systematic method for pull-in parameters calculation for the NEMS actuator is needed. The objective of this research is to develop a novel method for these above-mentioned NEMS parameters calculation. For this, the mechanical behavior of a clamped-clamped NEMS actuator is investigated based on a continuous Euler-Bernoulli beam model. To get the needed pull-in parameters, the nonlinear governing differential equation is to be solved numerically. Various methods can be used in this regards such as the Finite-Element Method [26], Finite-Difference Method [27], Shooting Method [28], [29], and Differential-Quadrature Method [27], etc., which are considered to be computationally expensive and in some cases unstable, since some rely on initial guesses. In this paper, we propose to use Galerkin-based reduced-order modeling that transforms the nonlinear governing differential equation into nonlinear algebraic equations system (for a static problem). Then, we propose to solve the nonlinear algebraic equations using some powerful numerical scheme. Our presented results show the efficiency and accuracy of the proposed method. The influence of the van der Waals force, the axial stress, and the fringing field effects are investigated on the pull-in parameters (gap and voltage) of a nano-actuator. The detachment length of the clamped-clamped nano-actuator is also examined.

In the coming sections, the governing equations of the proposed actuator are first presented. Then, description of the reduced-order model is presented. The static problem of the electrostatic actuator under a DC load are solved and discussed. And finally, the main results of this theoretical investigation are summarized in the conclusion section.

II. Problem Formulation

In this section, we formulate the model governing the mechanical behavior of an electrostatic actuator under the effect of van der Waals forces. We consider a flexible doubly-clamped prismatic nanobeam, Fig. 2 (a). The length of the beam is L, its cross-section area is $A = bh$, its second moment area is $I_{\hat{y}\hat{y}} = bh^3/12$, where b and h are the width and the thickness of the beam, respectively. The beam is assumed to be made of homogeneous isotopic linearly elastic material with density ρ, Young's modulus E and Poisson's ratio v. Since the width b of the microbeam is somehow larger than its thickness h, we suggest to use an effective modulus of elasticity $E' = E/2(1-v^2)$ [30].

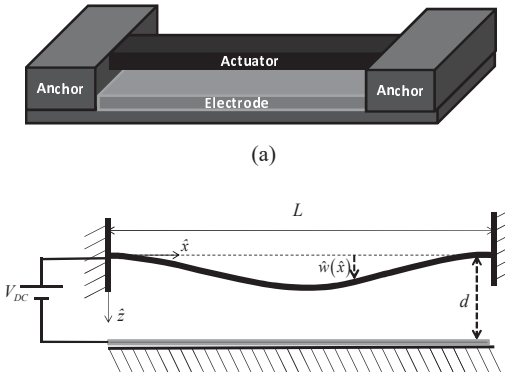

Fig. 2 (a) 3D schematic and (b) in- plane view of the electrostatically-actuated actuator

Hereafter, (ˆ) denotes dimensional quantities. The microbeam is free to deflect in the $(\hat{x},\hat{z})$ plane, while its clamped ends are constrained in both lateral $\hat{z}$ and axial $\hat{x}$ directions by unmovable anchors. The beam is actuated by an electrostatic force assumed to have only a $\hat{z}$ -component by a grounded electrode located underneath the beam and with an initial gap distance d in the $\hat{z}$ direction, Fig. 2 (b). The nanobeam is described in the framework of the Euler-Bernoulli theory, since we are assuming that h « L and that the deflections, while comparable with the thickness of the beam, are small with respect to the beam's length. In addition, we assume that the axial and rotary inertia are negligible compared with the transverse inertia. Under these common assumptions, (1), describing the in-plane static displacement $\hat{w}(\hat{x})$ of the above described actuator can be written as [31], [32].

$$E'I\frac{d^4\hat{w}}{d\hat{x}^4} = \frac{E'A}{2L}\left(\int_0^L\left(\frac{d\hat{w}}{d\hat{x}}\right)^2 d\hat{x}\right)\frac{d^2\hat{w}}{d\hat{x}^2} + \hat{F}_e\left(\hat{w},V_{DC}\right) + \hat{F}_{vdw}\left(\hat{w},\gamma_{vdw}\right), \quad (1)$$

where the functions $\hat{F}_e(\hat{w},V_{DC})$ and $\hat{F}_{vdw}(\hat{w},\gamma_{vdw})$ represent the distributed electrostatic force and the van der Waals force per unit length arising between the two parallel electrodes, respectively.

Considering the electric fringing-fields effect, the electrostatic force per unit length of the beam can be approximated as [33], [34]

$$\hat{F}_e(\hat{w},V_{DC})=\frac{\varepsilon_0 b V_{DC}^2}{2(d-\hat{w}(\hat{x}))^2}\left(1+0.65\frac{(d-\hat{w}(\hat{x}))}{b}\right), \quad (2)$$

where $\varepsilon_0 = 8.854\times10^{-12}$ $C^2N^{-1}m^{-2}$ is the permittivity of free space and V_{DC} is the DC voltage applied between the moving electrode and the stationary one separated by an initial gap distance of d.

The van der Waals force per unit length of for the considered nano-actuator can be approximated as [35].

$$\hat{F}_{vdw}(\hat{w},\gamma_{vdw})=\frac{\gamma_{vdw}Hb}{6\pi(d-\hat{w}(\hat{x}))}, \quad (3)$$

where $H = 4.4\times10^{-19}$ J is the Hamaker constant, and γ_{vdw} is an introduced detuning parameter, which is defined to be positive and not exceeding one. This book-keeping parameter will govern the importance of the van der Waals force: if it is close to zero, this means that the van der Waals force is of minimal amplitude, and hence negligible. If this coefficient is close to one, this means that the van der Waals force is at its maximum amplitude.

$$\hat{w}(0)=0, \quad \frac{d\hat{w}}{d\hat{x}}(0)=0, \quad \hat{w}(L)=0, \quad \frac{d\hat{w}}{d\hat{x}}(L)=0, \quad (4)$$

For convenience, we introduce the following non-dimensional variables:

$$w=\frac{\hat{w}}{d}, \qquad x=\frac{\hat{x}}{L}, \quad (5)$$

By substituting (5) into (1)-(4), the normalized equation of motion and associated boundary conditions for the considered clamped-clamped actuator are written as:

$$\frac{d^4w}{dx^4}=\alpha_s\left(\int_0^1\left(\frac{\partial w}{\partial x}\right)^2dx\right)\frac{\partial^2 w}{\partial x^2}+\frac{\alpha_e V_{DC}^2}{(1-\hat{w}(\hat{x}))^2}\left(1+0.65\frac{(1-\hat{w}(\hat{x}))}{\hat{b}}\right)+\frac{\alpha_{vdw}}{(1-\hat{w}(\hat{x}))}, \quad (6)$$

$$w(0)=0, \quad \frac{dw}{dx}(0)=0, \quad w(1)=0, \quad \frac{dw}{dx}(1)=0, \quad (7)$$

where

$$\alpha_s=\frac{Ad^2}{2I}=6\left(\frac{d}{h}\right)^2, \quad \alpha_e=\frac{\varepsilon_0 bL^4}{2E'Id^3}, \quad \alpha_{vdw}=\frac{\gamma_{vdw}HbL^4}{6\pi E'Id^2}, \quad \alpha_{fr}=\frac{b}{d}, \quad (8)$$

The solution of the nonlinear differential equation, (6)-(8), cannot be calculated analytically in a closed form, but will be approximated numerically in the next section.

III. Numerical Model

We propose here to solve the nonlinear problem of the electrostatic actuator, (6)-(8), in order to predict its pull-in parameters. There are various methods such as Finite-Elements Method (FEM), Finite-Difference Method (FDM), Reduced-Order Modeling (ROM) technique, etc., to solve such nonlinear equations. We propose here to use the latter approach. In this regards, (6)-(8) are discretized using the Galerkin procedure to yield a ROM [36]. Hence, the static deflection of the actuator is approximated as:

$$w(x)=\sum_{i=1}^{n}a_i\phi_i(x), \quad (9)$$

where $\phi_i(x)$ are the normalized linear undamped mode shapes of a clamped-clamped beam and a_i are the unknown constant coefficients for each respective assumed mode-shapes in the Galerkin discretization, (9). To obtain the ROM discretized equations, we substitute (9) into (6)-(8), multiply by $\phi_i(x)$, use the orthogonality conditions of the mode shapes, and then integrate the outcome from 0 to 1. This results in a system of nonlinear algebraic equations in terms of the unknown coefficients a_i. The system is then solved numerically using the Newton-Raphson method [37].

We should mention here that the mode shapes $\phi_i(x)$ will remain embedded inside the denominator of the electrostatic, as well as the van der Waals forces functions in the ROM equations. To deal with the complicated integral terms due to the nonlinear forces, we simultaneously evaluate the spatial integrals containing the mode shapes $\phi_i(x)$ numerically, while solving the algebraic equations with respect to the unknown coefficients a_i (11).

IV. Results

As a case study, we consider clamped-clamped MEMS and NEMS actuator, made both of Polysilicon respectively, and which the geometrical and material properties are summarized in Table I.

TABLE I
Geometrical and Material Properties of the Actuators

Symbol	MEMS Actuator Case	NEMS Actuator Case
b	50 μm	100 nm
h	3 μm	50 nm
E'	166 GPa	166 GPa
d	1 μm	50 nm
L	250-350 μm	12 μm

We start first by solving the problem considering the MEMS actuator case of Table I. We propose to compare our ROM results with two other distinct numerical methods. We first used a 3D FEM simulator, and then implemented a finite-difference scheme. We also assumed the case without the van der Waals effects, which are usually not prominent in the

MEMS scale. We should mention here that the FEM results were obtained through an ANSYS model, consisting of a coupled electrostatic-structural element (TRANS126 elements) to model the electrostatic coupling between the beam and a ground electrode. This element is a two nodes element which has one structural degree of freedom and an electrical potential between the nodes. One end of each element is held fixed, while the other is coupled to a structural node in the beam. A voltage difference is applied across the TRANS126 element, which creates an attractive force that is resisted by the stiffness of the beam. The FDM were implemented by discretizing the space domain (x) into $n+1$ points, while enforcing the boundary conditions around x_0 and x_m. Consequently, the space domain is discretized using n equally-spaced points. At each of these points, we have to write the nonlinear equation of motion. This yields a set of n nonlinear algebraic equations. Then, a two-step explicit central-difference scheme is used to approximate the space derivatives. The resultant equations can be solved for the deflection unknowns at each selected point using the Newton-Raphson method.

TABLE II
THE CALCULATED PULL-IN VOLTAGES FOR THE MEMS ACTUATOR OF TABLE I ASSUMING THREE DIFFERENT METHODS

Length	**ROM** (N=5 IN (9))	**FEM**	**FDM**
L=250 μm	20.4	20.7	20.1
L=350 μm	39.2	39.8	39.3

The results generated using all three distinct methods are summarized in Table II. We clearly notice from the table that five modes ROM results are in excellent agreement with the results of both FEM and FDM. This confirms that the proposed ROM method is converging without any numerical instability problems.

Now, we examine the convergence of the ROM as the number of modes is increased (increasing n in the Galerkin expansion, (9)). Fig. 3 shows the maximum static deflection of the NEMS actuator of Table I using one, four, and five modes in the ROM. Shown results were simulated while neglecting the stretching effect ($\alpha_s = 0$) and while taking both the van der wall and the electric fringing-fields effects into consideration (α_{vdw}, $\alpha_{fr} \neq 0$). It follows from Fig. 3 that using four modes in the ROM yields acceptable converged results. The same figure shows that the relationship between the maximum deflections becomes increasingly nonlinear when the voltage applied is increased.

The shown branches in Fig. 3 corresponds to stable equilibria of the system for a given $V_{DC} \in (0..V_{pull-in})$. Beyond a critical voltage denoted by $V_{pull-in}$, there are no equilibria. This critical point, known as the pull-in voltage, corresponds to 0.261 *Volt* and a maximum deflection of 14 *nm*. These values of the pull-in voltage and the maximum deflection at this voltage provide essential design criterion for electrically-actuated MEMS and NEMS devices as an upper limit for their structural stability.

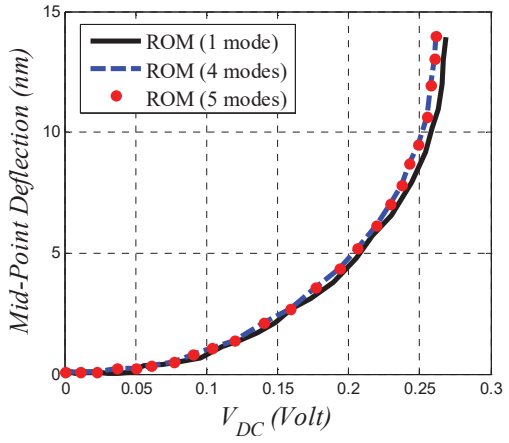

Fig. 3 Variation of the static displacement of the NEMS actuator with the applied DC load for different numbers of modes in the ROM

We propose now to investigate the effect of the van der Waals force and the electric fringing-fields on the above mentioned NEMS actuator design parameters. For this, we demonstrate the difference in the static profile of the NEMS actuator of Table I with and without considering those effects respectively in Figs. 4 and 5. It is noted from these two figures that both effects are affecting the values of voltage and actuator maximum deflection at the pull-in state.

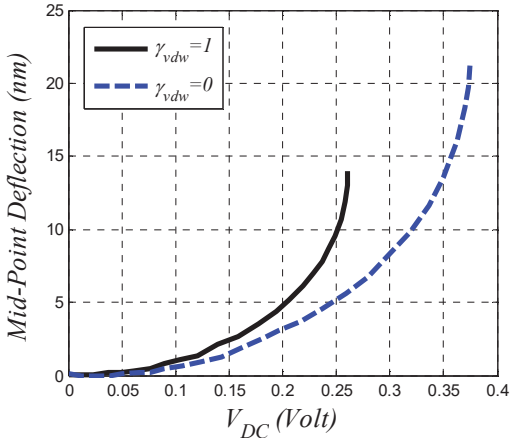

Fig. 4 Comparison of the maximum static deflection of the nano-actuator with the applied DC load while assuming van der Waals effect (solid black), and while neglecting it (dashed blue)

In fact, the van der Waals force is of attractive nature, it helped in increasing the nano-actuator static deflection and hence decreasing its pull-in voltage value, as well as the gap at this pull-in voltage, Fig. 4. Also, we can clearly see the influence of the electric fringing-fields on the static profile of the nano-actuator, Fig. 5. Again this effect is adding more amplitude to the attractive actuating electrostatic force, and hence increases the beam deflection. This reduced the pull-in

voltage while increasing slightly the beam deflection at the pull-in voltage.

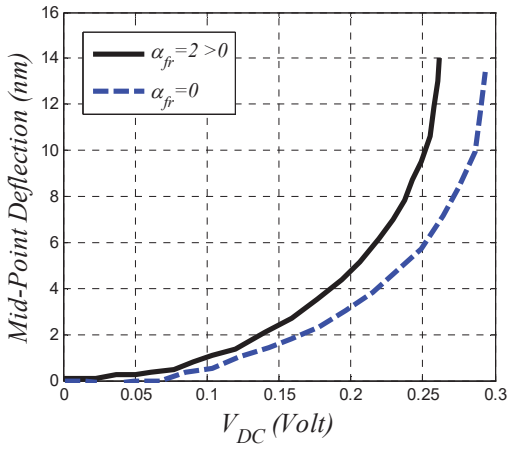

Fig. 5 Comparison of the maximum static deflection of the nano-actuator with the applied DC load while assuming electric fringing-fields effect (solid black), and while neglecting it (dashed blue)

One of the key and basic design parameters for NEMS actuators is the detachment length. It is by definition the maximum length of the nanobeam that will not stick to the actuating substrate, even without the application of any external voltage [24]. There are multiple ways to get this unstuck length of the nano-actuator. It can be obtained by increasing the actuator length until we reach an instability state for very small values of the applied DC voltage. For our case study of the NEMS actuator of Table I, we calculated numerically the detachment length to be equal to 16.79 μm, Fig. 7. This means that if we select any length for the actuator larger than 16.79 μm, the nanobeam will stick to the ground plane due to the attractive nature of the van der Waals force without the application of any DC voltage. The variation of the pull-in voltage versus length of the fixed-fixed end type NEMS actuator is depicted in Fig. 7. This process has been repeated for several gap distance values d, Fig. 8. The variation of the maximum length with the initial gap distance of the NEMS actuator is presented in Fig. 8. From both figures, if we know one of the two mentioned parameters, we can determine the other parameter in the way that the actuator does not adhere to the substrate due to the van der Waals force effect.

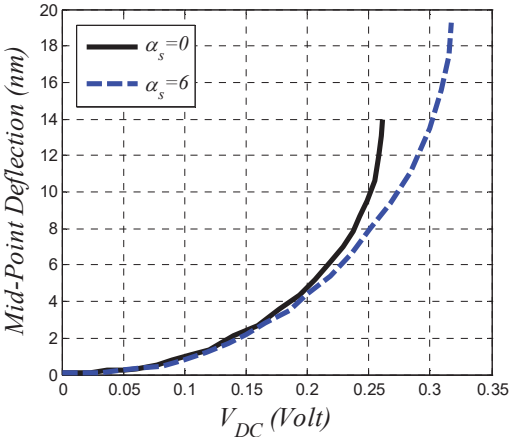

(a)

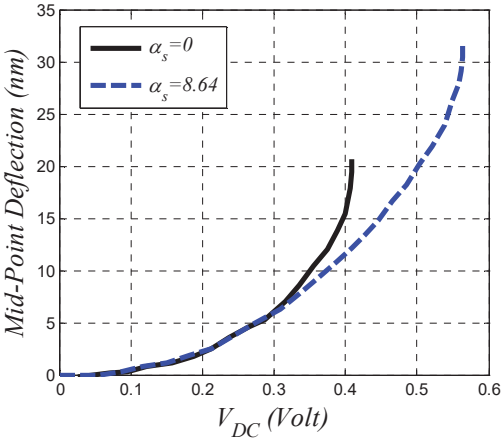

(b)

Fig. 6 Variation of the maximum static deflection of the nano-actuator with the applied DC load while assuming geometric nonlinearity (dashed blue), and while neglecting it (solid black), for an initial gap of (*a*) d= 50 nm, and (*b*) d= 60 nm, respectively.

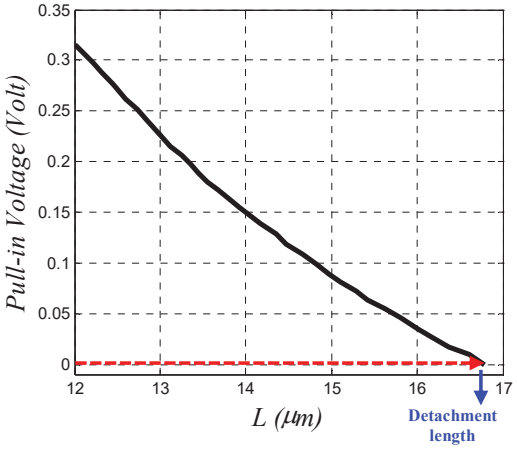

Fig. 7 Variation of the pull-in voltage with the length of the NEMS-actuator of Table I

Here, we intend to investigate the effect of the geometric nonlinearity of the NEMS actuator of Table I. The difference in the results between both models (one with considering the geometric nonlinearity and one with neglecting this effect) is illustrated in Figs. 6 and 7 for two different initial gaps, 50 *nm* and 60 *nm*, respectively. It is noted from these two figures that the geometric nonlinearity shows significant influence on the NEMS actuator pull-in parameters. As seen from both figures, the actuator with geometric nonlinearity responds at a deflection and voltage till pull-in larger compared to the one without geometric nonlinearity. This is consistent with the mid-plane stretching effect, due to the geometric nonlinearity, which acts as a repulsive (stiffening) force and which increases nonlinearly the stiffness of the actuator. Also, we can understand from Fig. 6, that by increasing the initial gap, the influence of the axial stress effect has been amplified.

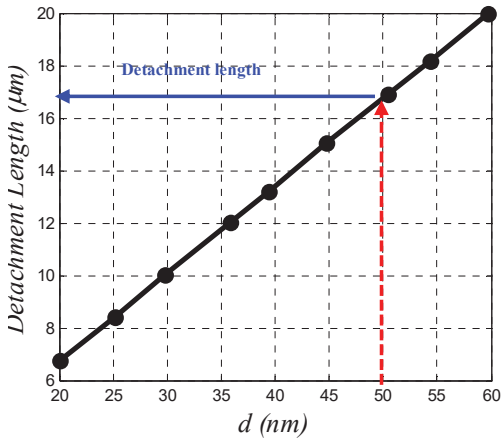

Fig. 8 Variation of calculated detachment length with the initial gap of the NEMS-actuator of Table I

V. Conclusion

In this paper, an investigation into the nonlinear static behavior of an electrically actuated clamped-clamped micro and nano-actuator was presented. A Euler-Bernoulli continuous beam model was adopted while considering the van der Waals force and the electric fringing-fields nonlinear effects. The geometric effect of midplane stretching was also taken into consideration in the proposed model. The nonlinear differential equation was discretized using a ROM obtained through a Galerkin expansion technique, and then solved numerically assuming the Newton-Raphson method. First, the numerical results were compared with the FEM and FDM methods, with the comparison showing excellent agreement. Then, the pull-in parameters of a nano-actuator were calculated while looking at the effects of all the nonlinear components such as: the electric fringing-fields, the midplane stretching (geometric nonlinearity), and the van der Waals force. The results showed that the van der Waals force and the electric fringing-field components decrease the pull-in voltage, while increasing the nano-actuator deflection at the pull-in state. The results also demonstrated that the geometric nonlinearity component increases the pull-in voltage while decreasing the nanobeam deflection. The detachment length of the actuator as a basic design parameter was also obtained. The results of the present paper can be used in the design and modeling of MEM/NEM actuators.

In the future, we plan to extend the study to solve the full dynamical behavior of such devices under AC harmonic loads. We also plan to study the influence of damping on vibrational amplitudes, while looking at any probability of dynamical instability regions.

Acknowledgment

The author would like to thank the Deanship of the Scientific Research (DSR) at King Fahd University of Petroleum and Minerals (KFUPM).

References

[1] G. T. A. Kovacs, *Micromachined Transducers Sourcebook*. McGraw-Hill, NY, 1998
[2] H. C. Nathanson, and R. A. Wickstrom, "A resonant gate silicon surface transistor with high Q bandpass properties," *IEEE Appl. Phys. Lett.*, vol.7, 1965, pp. 84-86.
[3] F. D. Bannon, J. R. Clark, and C.T.C. Nguyen, "High-Q HF Microelectromechanical Filters," *J. Solid-State Circuits*, vol. 35, 2000, pp. 512-526.
[4] T. P. Burg, A. R. Mirza, N. Milovic, C. H. Tsau, G. A. Popescu, J. S. Foster, and S. R. Manalis, "Vacuum-packaged suspended microchannel resonant mass sensor for biomolecular detection," *J. Microelectromech. Syst.*, vol. 15, 2006, pp. 1466-1476.
[5] W. T. Hsu, J. R. Clark, and C. T. C. Nguyen, "A resonant temperature sensor based on electrical spring softening", *Transducers 01, Eurosensors XV*, *The 11th International Conference on Solid-State Sensors and Actuators*, Munich, Germany, 2001.
[6] B. Kim, M. A. Hopcroft, R. Melamud, C. M. Jha, M. Agarwal, S. A. Chandorkar and T. W. Kenny, "CMOS compatible wafer-scale encapsulation with MEMS resonators", *ASME InterPACK*, Vancouver, Canada, 2007.
[7] T. Rueckes, K. Kim, E. Joselevich, G. Y. Tseng, C-L. Cheung, and Lieber C. M., "Carbon nanotube-based nonvolatile random access memory for molecular computing," *Science*, vol. 289, 2000, pp.94–97.
[8] M. Dequesnes, S. Tang, and N.R. Aluru, "Static and Dynamic analysis of carbon nanotube-based switches", *Transactions of the ASME*, vol. 126, 2004, pp. 230-237.
[9] P. G. Collins, K. B. Bradley, M. Ishigami, and A. Zettl, "Extreme oxygen sensitivity of electronic properties of carbon nanotubes," *Science*, vol. 287, 2000, pp. 1801–1804.
[10] C. K. W. Adu, G. U. Sumanasekera, B. K. Pradhan, H. E. Romero, and P. C., Eklund, "Carbon nanotubes: a thermoelectric nano-nose," *Chem. Phys. Lett.*, vol. 337, 20001, pp. 31-35.
[11] H. M. Ouakad, and M. I., Younis, "Nonlinear dynamics of electrically actuated carbon nanotube resonators," *Journal of Computational and Nonlinear Dynamics*, vol. 5, 2010, pp. 011009.
[12] A. F. Marquès, R.C. Castelló, and A.M. Shkel, "Modelling the Electrostatic Actuation of MEMS: State of the Art 2005", *Technical Report, IOC-DT*, Vol 18, 2005, pp 1-24.
[13] H. Nathanson, W. Newell, R. Wickstrom, and J.R. Davis, "The Resonant Gate Transistor," *IEEE Transactions on Electronics devices*, vol. 14, 1967, pp. 117-133.
[14] W. Newell, "Miniaturization of Tuning Forks," *Smithsonian/NASA Physics Query Form Science*, vol. 161, 1986, pp. 1320-1326.
[15] D. J. Ijntema, and H. A. C. Tilmans, "Static and Dynamic Aspects of an Air-gap Capacitor", *Journal of Sensors and Actuators*, vol. 35, 1992, pp. 121-128.
[16] P. M. Osterberg, S. D. Senturia, "M-TEST: a test chip for MEMS material property measurement using electrostatically actuated test structures," *J Microelectromech Syst*, vol. 6, 1997, pp. 107-118.
[17] L. Castañer, A. Rodriguez, J. Pons, and S. D. Senturia, "Pull- in Time-Energy Product of Electrostatic Actuators: Comparison of Experiments

with Simulation," *Journal of Sensors and Actuators A*, vol 27, 1999, pp. 263-269.
[18] O. Bochobza-Degani, and Y. Nemirovsky, "Modeling the pull-in parameters of electrostatic actuators with a novel lumped two degrees of freedom pull-in model," *Sensors and Actuators A*, vol. 97, 2002, pp. 569-578.
[19] S. Krylov, and R. Maimon. "Pull-in Dynamics of an Elastic Beam Actuated by Continuously Distributed Electrostatic Force," *Transactions of the ASME: Journal of vibration and acoustics*, vol. 126, 2004, pp. 332-342.
[20] A. H. Nayfeh, M. I. Younis, and E. M. Abdel-Rahman, "Dynamic Pull-in Phenomenon in MEMS Resonators," *Journal of Nonlinear Dynamics*, vol. 48, 2007, pp. 153-163.
[21] M. Dequesnes, S. V. Rotkin, and N. R. Aluru, "Calculation of pull-in voltages for carbon-nanotube-based nanoelectromechanical switches," *Nanotechnology*, vol. 13, 2002, pp. 120-131.
[22] T. Tang, A. Jagota, and C. Y., Hui, "Adhesion between single-walled carbon nanotubes," *Journal of Applied Physics*, vol. 97, 2005, pp. 074304-07431.
[23] T. Tang, A. Jagota, C. Y., Hui, N. and J. Glassmaker, "Collapse of single-walled carbon nanotubes," *Journal of Applied Physics*, vol. 97, 2005, pp. 074310-074311.
[24] W-H. Lin, and Y.P. Zhao, "Nonlinear behavior for nanoscale electrostatic actuators with Casimir force," *Chaos, Solitons and Fractals*, vol. 23, 2005, pp. 1777-1785.
[25] G. W. Wang, Y. Zhang, and Y. P. Zhao, "Pull-in instability study of carbon nanotube tweezers under the influence of van der Waals forces," *Journal of Micromechanics and Microengineering*, vol. 14, 2004, pp. 1119-1125.
[26] H. S. Elmer, and S. D. Senturia, "Generating efficient dynamical models for microelectromechanical systems from a few finite-element simulation runs," *Journal of Microelectromechanical Systems*, vol. 8, 1999, pp. 280-289.
[27] F. Najar, S. Choura, E. M. Abdel-Rahman, S. El-Borgi, and A. H. Nayfeh, "Dynamic analysis of variable-geometry electrostatic microactuators," *Journal of Micromechanics and Microengineering*, vol. 16, 2006, pp. 2449.
[28] A. H. Nayfeh, M. I. Younis, and E. M. Abdel-Rahman, "Characterization of the mechanical behavior of an electrically actuated microbeam," *Journal of Micromechanics and Microengineering*, vol. 12.6, 2002, pp. 759-763.
[29] H. M. Ouakad, and M. I. Younis, "Modeling and Simulations of Collapse Instabilities of Microbeams due to Capillary Forces," *Hindawi Mathematical Problems in Engineering,* vol. 2009, 2009, pp. 1-16.
[30] M. I. Younis, and A. H. Nayfeh, "A study of the nonlinear response of a resonant microbeam to an electric actuation," *Nonlinear Dynamics*, vol. 31, 2003, pp. 91-117.
[31] G. J. Simitses, and D. H. Hodges, *Fundamentals of Structural Stability*, Elsevier, Amsterdam, 2006.
[32] A. H. Nayfeh, *Nonlinear Interactions*, Wiley Interscience, New York, 2000.
[33] R. K. Gupta, *Electrostatic pull-in test structure design for in-situ mechanical property measurements of microelectromechanical systems*, *PhD Thesis*, MIT, MA: Cambridge, 1997.
[34] J. M. Huang, K. M. Liew, C. H. Wong, S. Rajendran, M. J. Tan, and A. Q. Liu, "Mechanical design and optimization of capacitive micromachined switch," *Sensors and Actuators A*, vol. 93, 2001, pp. 273-285.
[35] J. N. Israelachvili, "Intermolecular and surface forces," Academic, London, 1992.
[36] H. M. Ouakad, "An electrostatically actuated MEMS arch band-pass filter," Shock and Vibration, vol. 20, 2013, pp. 809-819.
[37] E. T. Whittaker, and G. Robinson, "The Newton-Raphson Method," §44 in the Calculus of Observations: A Treatise on Numerical Mathematics: 4th edition, NY: Dover, pp. 84-87, 1967.

Hassen M. Ouakad was born in Bizerte (Tunisia) in November 1983. He received the B.Sc. degree, with honors, in Mechanics and Structures in 2007 from Tunisia Polytechnic. In 2008 he received a master degree in Computational Mechanics from a joint Graduate Program (CMGP) between Tunisia Polytechnic, Tunisia, and Virginia Tech, VA, USA. Then he joined the MEMS characterization and Motion Lab of the State University of New-York at Binghamton (NY, ISA), where he received the Ph.D. degree in 2010. In January 2011, he joined the Petroleum Engineering Department of the Texas A&M, Qatar as a postdoc research assistant. In September 2011 he joined the Mechanical Engineering Department of King Fahd University as an Assistant Professor.

Dr. Ouakad is the recipient of the 2010 Excellence in Research award granted by the Watson School of the State University of New-York at Binghamton, NY, USA. Dr. Ouakad holds two patents dealing with introducing new techniques for controlling the micro-contact printing in roll-to-roll processes. Furthermore, Dr. Ouakad designed new miniaturized devices that rely on the fringing-fields electric loads as an actuation technique in MEMS devices. Dr. Ouakad authored and co-authored more than fifty scientific articles published in highly ranked international journals and conferences. His work has been cited more than 400 times and his H index is 10.

Dr. Ouakad is a member in the Institute of Electrical and Electronic Engineers (IEEE), and the American Society of Mechanical Engineering (ASME). He currently serves as an Associate Editor for International Journal of Applied Mechanics and Engineering (IJAME) and has served on the scientific committees of several international conferences.